

Control Engineering Practice 8 (2000) 1237-1248

CONTROL ENGINEERING PRACTICE

www.elsevier.com/locate/conengprac

Estimation and control of mechatronic systems using sensitivity bond graphs[☆]

Peter J. Gawthrop^{a,*}, Eric Ronco^b

^aDepartment of Mechanical Engineering, Centre for Systems and Control, University of Glasgow, Glasgow G12 8QQ, Scotland, UK

^bInstitut d'Automatique, EPFL, 1015 Lausanne, Switzerland

Received 10 January 2000; accepted 31 March 2000

Abstract

A new bond graph framework for sensitivity theory is applied to model-based predictive control, state estimation, and parameter estimation in the context of physical systems. The approach is illustrated using a nonlinear mechatronic system. © 2000 Elsevier Science Ltd. All rights reserved.

Keywords: Bond graphs; Sensitivity; Optimisation; Predictive control; Parameter estimation

1. Introduction

This paper combines a number of ideas to give a new adaptive model-based output feedback controller applicable to practical non-linear systems. The key ideas used are:

- bond graph modelling (Karnopp, Margolis & Rosenberg, 1990; Thoma, 1990; Cellier, 1991; Gawthrop & Smith, 1996),
- sensitivity bond graphs (Cabanellas, Felez & Vera, 1995; Gawthrop, 2000),
- optimisation (Fletcher, 1987; Press, Teukolsky, Vetterling & Flannery, 1992),
- predictive pole-placement control (Gawthrop & Ronco, 1999),
- intermittent control (Ronco, Arsan & Gawthrop, 1999),
- partially known system identification (An, Atkeson & Hollerbach, 1988; Canudas de Wit, 1988; Dasgupta, Anderson & Kaye, 1986; Gawthrop, Jones & Mackenzie, 1992; Gawthrop, Ježek, Jones & Sroka, 1993).

Bond graphs provide a well-established technique for modelling dynamic systems; details may be found in the textbooks of Karnopp et al. (1990), Thoma (1990), Cellier (1991) and Gawthrop and Smith (1996). As a graphical approach, a number of computer-based graphical bond graph modelling tools have appeared including MTT (2000) — the one used to implement the ideas contained in this paper. The bond graph approach can be compared and contrasted with other methods under a number of different headings. Firstly, bond graphs are equation based (as opposed to assignment statement based). They share this property with approaches such as Modelica (2000) and Ascend (1999); but for this reason, the approach is superior to block diagram-based approaches such as Simulink. Secondly, they provide an energy-based approach which not only allows multi-domain modelling but ensures that the resultant model is energetically correct.

The bond graph approach has previously been suggested as a basis for control design by Karnopp (1979, 1995) and by Gawthrop (1995b). This paper develops the idea of *sensitivity* bond graphs (Cabanellas et al., 1995; Gawthrop, 2000) to provide a basis for model-based optimisation for the control and estimation of nonlinear dynamic systems for which a bond graph model is available. In so doing, it leads on to a bond-graph-based computer environment which seemlessly combines bond graph tools ranging from modelling and model-based control design through to real-time identification and control.

The sensitivity theory of dynamic systems and its application is well established and summarised in the

^{*}Extended version submitted to 1st IFAC Conference on Mechatronic Systems, Darmstadt, September 2000.

^{*}Corresponding author. Tel.: + 44-141-330-4960; fax: + 44-141-330-4343.

E-mail addresses: p.gawthrop@eng.gla.ac.uk (P.J Gawthrop), eric.ronco@epfl.ch (E. Ronco).

textbooks of Tomović and Vukobratović (1972) and Frank (1978). There are many applications of sensitivity methods to systems and control problems including system optimisation (Cabanellas et al., 1995), controller tuning (Van Amerongen & Udink ten Cate, 1975; Winning, El-Shirbeeny, Thompson & Murray-Smith, 1977; Oppen, Gong & Murray-Smith, 1995) and parameter estimation (Eykhoff, 1974). The particular class of dynamic systems described by electrical networks has its own techniques (Calahan, 1972) based on the adjoint circuit approach. In contrast to standard sensitivity theory (Tomović & Vukobratović, 1972; Frank, 1978), which operates at the system ordinary differential equation level, bondgraph-based sensitivity models (Cabanellas et al., 1995; Gawthrop, 2000) operate at the modelling level. In the special case of linearisation, Karnopp (1977) has stated: "Rather than treating linearized systems as abstract sets of equations, we here look for structural analogies between non-linear components relating total system variables and linearized models relating incremental system variables"; with "linearized" replaced by "sensitivity" this statement summarises the approach of Gawthrop (2000) used as a basis for this paper.

Optimisation has always been a fundamental technique in control and estimation of dynamic systems, and this has been become even more so with the popularity of model-based predictive control (MPC) (Clarke, 1994; Muske & Rawlings, 1993; Gawthrop, Demircioglu & Siller-Alcala, 1998; Chen & Allgöwer, 1998; Kouvaritakis, Cannon & Rossiter, 1999; Gawthrop & Ronco, 1999). Such methods rely on a *model* of the corresponding physical system. In some application areas (for example process control) physical, or first principles, models are hard to come by and so empirical models tend to be used. However in other application areas, in particular mechatronics, physical models are more readily available.

The predictive pole-placement (PPP) control introduced by Gawthrop and Ronco (1999) embeds the classical pole-placement state feedback design into a model-predictive formulation. This provides an alternative to model-predictive controllers which are based on linear-quadratic control. Although developed and analysed in a linear systems context, this paper shows that the method is applicable in the nonlinear case as well. As with any continuous-time method, there is a computational/real-time issue. This is solved using the *intermittent* approach of Ronco et al. (1999).

Whilst the emphasis in the paper is on systems that have a well-defined associated physical model, within this structure two forms of uncertainty are allowed: uncertain *states* and uncertain *physical parameters*. The identification of such *partially known* systems has a long history (An et al., 1988; Canudas de Wit, 1988; Dasgupta et al., 1986; Gawthrop et al., 1992, 1993) which has been given an sensitivity bond graph interpretation by

Gawthrop (2000). The state estimation is used to convert the *state* feedback predictive pole-placement to an *output* feedback algorithm.

The outline of the paper is as follows. Section 2 reviews the sensitivity of systems described by bond graphs and derives some results for the particular bond graph components used in this paper. Section 4 considers nonlinear model-based predictive control based on the linear predictive pole-placement of Gawthrop and Ronco (1999) and model-based parameter and state estimation. Section 5 illustrates the approach using a detailed model of, and data from, a laboratory inverted pendulum experiment. Section 6 makes some concluding remarks.

2. Sensitivity bond graphs

Sensitivity bond graphs are discussed by Cabanellas et al., (1995) and by Gawthrop (2000), and the closely related topic of linearised system bond graphs are discussed by Karnopp (1977). This section provides a brief introduction to the subject together with details relevant to this paper.

A bond graph component is associated with a *constitutive relationship* (or CR) which relates n_{v_i} time-varying *signals* within the component and n_{θ} time-invariant *parameters* associated with the system within which the component lies. Thus the CR for the *i*th component of a system can be written as

$$\Phi_i(v_i(t), \theta) = 0, \tag{1}$$

where $v_i \in \Re^{n_{e_i}}$ contains the *component* signals and $\theta \in \Re^{n_{\theta}}$ contains the *system* parameters.

In the special case that the CR is linear, it can be written as

$$A_i(\theta)^{\mathrm{T}} v_i(t) = 0, \tag{2}$$

where the time-invariant vector $A_i(\theta) \in \Re^{n_{vi}}$.

In this paper, the *sensitivity* ${}^{j}v_{i} \in \Re^{n_{vi}}$ of the signal vector v_{i} with respect to any (jth) component θ_{j} of the parameter vector θ is of interest. In particular, ${}^{j}v_{i}$ is defined as

$${}^{j}v_{i} = \frac{\partial v_{i}}{\partial \theta_{i}}.$$
(3)

It follows from Eq. (1) that $d\Phi_i(v_i(t), \theta)/d\theta = 0$ and so the sensitivity CR $\phi_i(^jv_i(t), v_i(t), \theta)$ becomes

$$\phi_{i}({}^{j}v_{i}(t), v_{i}(t), \theta) = \frac{\partial \Phi_{i}(v_{i}(t), \theta)^{\mathrm{T}}}{\partial v_{i}} {}^{j}v_{i}(t) + \frac{\partial \Phi_{i}(v_{i}(t), \theta)}{\partial \theta_{j}} = 0.$$

$$(4)$$

Eq. (4) is the sensitivity CR with respect to the *j*th parameter. It has the following important properties:

(1) The first term on the right-hand side of Eq. (4) represents the *linearised* (about $v_i(t)$) CR relating the sensitivity functions ${}^jv_i(t)$. In other words, it is a *linear* CR modulated by the variables $v_i(t)$ associated with the system itself. It can be written as the summation

$$\frac{\partial \Phi_i(v_i(t), \theta)^{\mathrm{T}}}{\partial v_i}^j v_i(t) = \sum_{k=1}^{n_{v_i}} \frac{\partial \Phi_i(v_i(t), \theta)^{\mathrm{T}}}{\partial v_{ik}} v_{ik}^j(t), \tag{5}$$

where v_{ik} and v_{ik}^{j} are the kth components of the vectors v_{i} and $^{j}v_{i}$, respectively.

- (2) The second term on the left-hand side of Eq. (4) represents an additional input to the sensitivity CR dependent on the variables $v_i(t)$ associated with the system itself.
- (3) The sensitivity CR of Eq. (4) is *local* to the component in the sense that the only variables appearing in Eq. (4) are $v_i(t)$ and ${}^jv_i(t)$.
- (4) The *j*th sensitivity CR of Eq. (4) does *not* depend on ${}^{l}v_{i}(t)$ for $l \neq j$.
- (5) If the *i*th CR $\Phi_i(v_i(t), \theta)$ does not depend on θ_j then the second term of Eq. (4) is zero and there is no *explicit* coupling between the actual and sensitivity systems (though there will be *implicitly* if $\Phi_i(v_i(t), \theta)$ is nonlinear). The corresponding sensitivity component is then the *linearised* component (Karnopp, 1977).
- (6) If $\Phi_i(v_i(t), \theta)$ is *linear* in v_i (Eq. (2)), then Eq. (4) becomes

$$A_i^{\mathsf{T}}(\theta)^j v_i(t) + \frac{\partial A_i^{\mathsf{T}}(\theta)}{\partial \theta_i} v_i(t) = 0. \tag{6}$$

- (7) If the conditions of both items (5) and (6) hold, then the CRs of the actual and sensitivity components are identical and uncoupled.
- (8) The bond graph sensitivity component can itself be represented by a bond graph comprising
 - (a) the original component corresponding to Eq. (1),
 - (b) the linearised component corresponding to the first term on the right-hand side of Eq. (4) and
 - (c) a coupling component corresponding to the second term on the right-hand side of Eq. (4).

An example of this appears in Fig. 1.

For these reasons, it is possible to encapsulate two CRs: the system CR of Eq. (1) and the *j*th sensitivity CR of Eq. (4) within a single component containing $2n_{v_i}$ variables: those contained in v_i and j_v . If the original component had N ports, the new sensitivity component (s-component) therefore has 2N ports. More conveniently, each port on the original component is replaced by a sensitivity port (or s-port) which carries not only the effort/flow pair e and f but also the corresponding sensi-

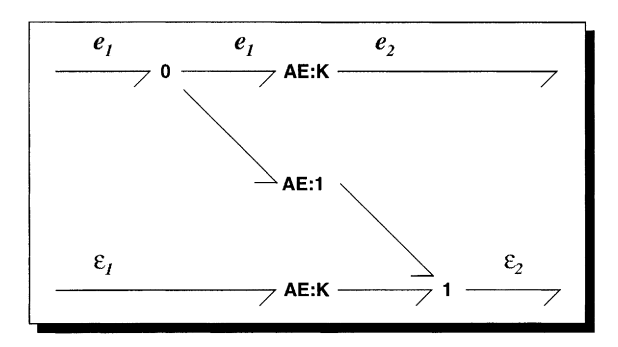


Fig. 1. The sensitivity component sAE.

tivity pair ${}^{j}e$ and ${}^{j}f$. Such ports may be considered to be connected by a *sensitivity bond* (s-bond) which encapsulates the energy bond carrying e and f with the pseudobond carrying e and e

It follows from the above equations that any bond graph component has an s-component equivalent. Moreover, if the corresponding component is *not* dependent on θ , it is then the *linearised* component as discussed by Karnopp (1977).

The following two examples are used in the paper.

2.1. A linear one-port R component

The standard linear bond graph \mathbf{R} component has a single port with effort e and flow f covariables related by the CR,

$$\Phi_i(v_i(t), \theta) = A_i(\theta)^{\mathrm{T}} v_i(t) = e - rf = 0.$$
(7)

That is, in the notation of Eq. (2),

$$A_i(\theta) = \begin{pmatrix} 1 \\ -r \end{pmatrix}, \qquad v_i = \begin{pmatrix} e \\ f \end{pmatrix},$$
 (8)

 $\partial A_i^{\mathsf{T}}(\theta)/\partial \theta_j = (0 - 1)^{\mathsf{T}}$ and so the sensitivity CR of Eq. (6) can be written as

$$\frac{\partial e}{\partial r} - r \frac{\partial f}{\partial r} - f = 0. \tag{9}$$

2.2. A linear amplifier AE component

The nonstandard linear bond graph **AE** component has two ports with effort e_1 and e_2 variables related by the CR,

$$\Phi_i(v_i(t), \theta) = A_i(\theta)^{\mathrm{T}} v_i(t) = e_2 - Ke_1 = 0.$$
 (10)

As this represents an ideal effort amplifier, the input flow $f_1 = 0$.

That is, in the notation of Eq. (2)

$$A_i(\theta) = \begin{pmatrix} 1 \\ -K \end{pmatrix}, \qquad v_i = \begin{pmatrix} e_2 \\ e_1 \end{pmatrix}, \tag{11}$$

 $\partial A_i^{\rm T}(\theta)/\partial \theta_j = (0 - 1)^{\rm T}$ and so the sensitivity CR of Eq. (6) can be written as

$$\frac{\partial e_2}{\partial K} - K \frac{\partial e_1}{\partial K} - e_1 = 0. \tag{12}$$

The first two terms of Eq. (12) correspond to the linear system itself, and the third term corresponds to the sensitivity.

Fig. 1 gives the bond graph corresponding to the sensitivity component **sAE**. The upper part of the diagram comprises the *actual* **AE** component with gain K and with CR given by Eq. (10). The lower part of the diagram corresponds to the *sensitivity* CR where $\varepsilon_i \equiv \partial e_i/\partial K$. The additional term (e_1) of Eq. (12) is represented by the middle unit gain **AE** component.

3. Optimisation

The algorithms for estimation and control considered in this paper give rise to optimisation problems of the form

$$\min_{\theta} J(\theta, t), \tag{13}$$

where $\theta \in \Re^{n_{\theta}}$ is the *parameter vector* and the *cost function* $J(\theta, t)$ is

$$J(\theta, t) = \frac{1}{2} \int_0^T e^{\mathsf{T}}(t, \tau) Q(\tau) e(t, \tau) \, \mathrm{d}\tau \tag{14}$$

where $Q(\tau) \in \Re^{n_y \times n_y}$ is a positive-semi-definite weighting function and the error $e(t, \tau) \in \Re^{n_y}$ is

$$e(t,\tau) = [y(t,\tau,\theta) - z(t,\tau)]. \tag{15}$$

 $y(t, \tau, \theta) \in \Re^{n_y}$ is the system output and $z(t, \tau) \in \Re^{n_y}$ a function of time. In general, y is *not* linear in θ and so $J(\theta, t)$ is *not* in general quadratic in θ .

This paper is concerned with real-time control and estimation and so optimisation speed is of the essence. Therefore, rapid convergence combined with simplicity is desirable. As, using the sensitivity bond graph approach, gradient information is cheaply available, this suggests the use of methods which make use of gradient information. For these reasons, out of the plethora of methods available (see, for example, the book of Press et al., 1992), the quasi-Newton method was chosen. Further research may yield alternative choices, but the experience so far has been good. In particular, as shown by Ronco and Gawthrop (1999) this approach is much faster than nonlinear programming methods which do not use derivative information.

Differentiation of Eqs. (13) and (15) with respect to θ relate the gradient J_{θ} of J (with respect to θ) to the corresponding gradient $y_{\theta}(t)$ and the output y(t) as

$$J(\theta, t)_{\theta} = \int_{0}^{T} [y(t, \tau, \theta) - z(t, \tau)]^{T} Q(\tau) y_{\theta}(t, \tau) d\tau$$
 (16)

The quasi-Newton approach approximates the second derivative $J(\theta, t)_{\theta\theta}$ of the cost function by

$$J(\theta, t)_{\theta\theta} \approx \hat{J}(\theta, t)_{\theta\theta} = \int_0^T y_{\theta}(t, \tau) Q(\tau) y_{\theta}^{\mathsf{T}}(t, \tau) \, \mathrm{d}\tau. \tag{17}$$

As discussed by Gawthrop (2000) (and summarised in Section 2) the optimisation algorithm is then to repeatedly compute

$$\theta := \theta - \Delta \theta \tag{18}$$

until some convergence criterion is satisfied where $\Delta\theta$ is the solution of the set of linear equations:

$$\hat{J}_{\theta\theta}\Delta\theta = J_{\theta}.\tag{19}$$

Two simple modifications of this method give additional robustness in the face of difficult optimisation problems (Press et al., 1992):

- (1) Eq. (19) is solved via a singular-value decomposition based pseudo-inverse and
- (2) A check is made that the cost function decreases at each step; if it does not, the step length is multiplied by the scalar $0 < \beta < 1$ (whilst retaining the step direction) until it does.

Finally, it is worth emphasising that the optimisation algorithm attempts to minimise the square of a *nonlinear* function with the help of the sensitivity (linearised) system — the sensitivity system is *not* itself optimised.

4. Model-based estimation and control

There are many approaches to model-based predictive control including those described by Muske and Rawlings (1993), Gawthrop et al. (1998), Chen and Allgöwer (1998) and Kouvaritakis et al. (1999).

However, the recently developed method of Gawthrop and Ronco (1999) is particularly appropriate to the sensitivity bond graph theme of this paper; however, this does not exclude the possibility of bringing other methods within the same framework. This method is briefly described in Section 4.1.

In common with many model-based predictive control, the one described in Section 4.1 is a *state* feedback method. Therefore, to give *output* feedback, Section 4.2 develops a simple, but novel, nonlinear observer which can be used for parameter, as well as state, estimation.

These two algorithms are brought together within the intermittent control context discussed by Ronco et al. (1999) to give the overall implementable algorithm in Section 4.3.

4.1. Model-based predictive control

Much work on model-based predictive control is in a discrete-time setting and therefore inappropriate to the context of this paper. However, a number of continuoustime approaches are available including those of Demircioglu and Gawthrop (1991), Gawthrop et al. (1998) and Chen and Allgöwer (1998). More recently, a new approach *predictive pole placement* (PPP) has been developed by Ronco (1999) which, although for linear systems, readily extends to this nonlinear context.

The nonlinear systems considered in this paper are represented by

$$E(x)\frac{\mathrm{d}x}{\mathrm{d}t} = f(x, u),$$

$$y = g(x).$$
(20)

Such constrained-state equations can be derived directly from the system bond graph (Gawthrop & Smith, 1996). In simple cases E(x) = I, the unit matrix, in which case Eq. (20) is in standard ordinary differential equation form. In typical mechatronic systems, $E(x) > 0 \ \forall x$. Despite the fact that Eq. (20) could be then rewritten as

$$\frac{\mathrm{d}x}{\mathrm{d}t} = f_e(x, u),$$

$$y = g(x),$$

$$f_e(x, u) = E^{-1}(x)f(x, u),$$
(21)

it is often better to work with Eq. (20) directly as the inverse of E(x) can be a complicated algebraic expression.

As in the linear case discussed by Gawthrop and Ronco (1999) (and many other model-based predictive controllers), interest lies in the solutions of

$$E(x^{\star}(t,\tau))\frac{\mathrm{d}}{\mathrm{d}\tau}x^{\star}(t,\tau) = f(x^{\star}(t,\tau), u^{\star}(t,\tau)),$$

$$y^{\star}(t,\tau) = g(x^{\star}(t,\tau)).$$
 (22)

The differential Eqs. (20) and (22) are related by having the *same* state-space matrices and by imposing the *cross-coupling* conditions:

$$x^*(t,0) = x(t),$$

 $u(t) = u^*(t,0).$ (23)

As in the approach of Gawthrop and Ronco (1999), the moving horizon control signal $u^*(t,\tau)$ is linearly parameterised by the n_U components of the column vector U(t) so that

$$u^{\star}(t,\tau) = U^{\star}(\tau)U(t),\tag{24}$$

where $U^*(\tau)$ is a $n_u \times n_U$ matrix of functions of τ . For the purposes of this paper, the particular $U^*(\tau)$ given by

$$U^{\star \mathsf{T}}(\tau) = \mathrm{e}^{A_u \tau} U_0 \tag{25}$$

is chosen, that is $U^{\star T}(\tau)$ is the state of the autonomous system

$$\frac{\mathrm{d}}{\mathrm{d}\tau} U^{\star \mathrm{T}}(\tau) = A_u U^{\star \mathrm{T}}(\tau),$$

$$U^{\star}(0) = U_0^{\mathrm{T}}.$$
(26)

The components of $U^*(\tau)$ can be regarded as a set of *basis* functions for the control signal $u^*(t,\tau)$ and the components of U(t) the corresponding weights or tuneable parameters. This idea is equally applicable to the nonlinear case.

Similarly, the *moving horizon* setpoint $w^*(t, \tau)$ is linearly parameterised by the n_W components of the column vector W(t) so that

$$w^{\star}(t,\tau) = W^{\star}(\tau)W(t),\tag{27}$$

where $W^{\star}(\tau)$ is a $n_y \times n_W$ matrix of functions of τ . Typically, the components $W_i^{\star}(\tau)$ of $W^{\star}(\tau)$ will be constant:

$$W_i^{\star}(\tau) = \begin{cases} 1 & \text{for tracking,} \\ 0 & \text{for regulation.} \end{cases}$$
 (28)

In the particular case of predictive control, the optimisation cost $J(\theta)$ is of the form of Eqs. (13) and (14) where $T=T_2$ is the upper time horizon, $\theta=U(t)$ and $z(t,\tau)=w^*(t,\tau)$. The weighting function Q(t) is

$$Q(t) = \begin{cases} 0_{n_y} & \text{if } t \leqslant T_1, \\ I_{n_y} & \text{if } t > T_1, \end{cases}$$

$$(29)$$

where 0_{n_y} and I_{n_y} are the $n_y \times n_y$ zero and unit matrices, respectively. As discussed by Gawthrop and Ronco (1999), the aim of this cost is to make the system output as close to the setpoint as possible between times T_1 and T_2 whilst ignoring initial transient behaviour.

Unlike the linear case, the cost function $J(\theta,t)$ will no longer be necessarily quadratic in U(t) and so explicit minimisation is no longer possible. However, numerical optimisation is simplified if the derivative $J_{\theta}(\theta,t)$ is available. Computation of $J_{\theta}(\theta,t)$ requires, in turn, the computation of $y_{\mathcal{U}}^{\star}(\tau)$; this is precisely the information available from the sensitivity bond graph.

4.1.1. Bond graph interpretation

Here, a new sensitivity bond graph interpretation of the approach of Gawthrop and Ronco (1999) is given. The discussion is restricted to the single input case ($n_u = 1$) assuming that the input is an effort, but can readily be extended to the more general case.

Eq. (24) is the core of PPP and thus giving a bond graph representation of this equation is a key issue. This bond graph representation is given for the case when

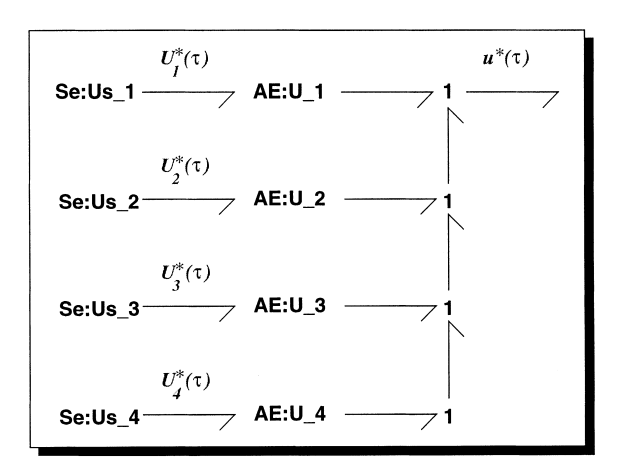


Fig. 2. Open-loop control.

 $n_U = 4$ in Fig. 2. The individual parts of Eq. (24) are the given bond graph interpretations as follows.

U(t): Each element of the (adjustable) weight vector U(t) ($U_i(t)$) is interpreted as the *gain* of a bond graph amplifier (**AE**) component (see Section 2.2).

 $U^*(\tau)$: The corresponding element of the basis function vector $U^*(\tau)$ ($U_i^*(\tau)$) is interpreted as the output of a bond graph source Se component which acts as the input of the corresponding AE component. (The Se, as opposed to the modulated MSe source component, is appropriate here as it represents a fixed function of time as specified by, for example, Eq. (25).)

Thus, the output of each **AE** component represents the *product* of $U_i(t)$ and $U_i^{\star}(\tau)$; these products are then *summed* at a **1** junction to implement the scalar product implied by Eq. (24).

With this interpretation, the problem of determining the sensitivity $y_v^*(\tau)$ of the system output $y^*(t,\tau)$ of the dynamic system of Eq. (22) with respect to the weighting vector U(t) is interpreted as finding the sensitivity bond graph corresponding to the bond graph of the dynamic system augmented by the bond graph of Fig. 2.

In particular, using the sensitivity bond graph approach of Section 2, the bond graph of Fig. 2, together with the rest of the dynamic system, is converted into a sensitivity bond graph, thus giving the *sensitivity* of the system outputs with respect to each of the n_U amplifier $gains - n_U$ components of U(t) required for Eqs. (16) and (17).

4.2. Parameter and state estimation

Each bond graph component has a constitutive relationship containing a number of *parameters*. Thus, for example, the **R** component with CR of Eq. (7) is parameterised by r. Because of the close mapping of the bond

graph to the corresponding physical system, each such parameter has a precise physical meaning. Many of these parameters (such as lengths and masses) will be known a priori from data sheets or physical inspection; others such as friction coefficients will not be precisely known.

Therefore, many systems will be *partially known* in this sense. Such systems are typically not linear in the system parameters and various approaches to this issue are described elsewhere (Dasgupta et al., 1986; Canudas de Wit, 1988; Gawthrop et al., 1992). Here, an off-line optimisation approach based on Section 3 is adopted.

The signal $z(t, \tau)$ of Eq. (15) is defined as

$$z(t) = y_m(t+\tau), \tag{30}$$

where $y_m(t)$ is the *measured* actual system output. The parameter vector θ contains the system parameters. The weighting function Q is

$$Q(t) = I_{n_y} \tag{31}$$

giving equal weighting to the parameter error.

As noted previously by Gawthrop (1995a), the initial state of a dynamic system represented by a bond graph may be explicitly represented by the addition of an **Se** component to the corresponding **C** components and an **Sf** component to the corresponding **I** components. Thus, the initial state translates to a system parameter — the value of the source output — and so these parameter identification techniques can be applied equally well to initial state estimation.

4.3. The intermittent approach

Continuous-time predictive control algorithms have the apparently fatal drawback that optimisation must be completed within an infinitesimal time. However, this problem can be overcome using intermittent control; see, for example, Ronco et al. (1999) for a detailed discussion of the approach.

Briefly, the idea is to update the control weights *intermittently*, and, during this time T_{ol} , run the controller in open loop using the previously calculated trajectory. Thus, there are two processes running in parallel: generation of the open-loop control and computation of the control weights U(t) ready for the *next* open-loop control trajectory. Thus, control is continuous but feedback is intermittent: this has biological analogies.

As discussed by Gawthrop & Ronco (1999), the PPP optimisation problem can be solved explicitly or, if computed recursively, the quasi-Newton algorithm converges in a single step. However, in the nonlinear case, convergence can take many steps depending on the initial choice of $\theta = U(t)$. Therefore, the choice of the initial value is important to ensure rapid convergence. In the linear case, it is known that, in the absence of disturbances, the open- and closed-loop trajectories are the same and thus the open-loop control trajectory in one

interval is the *continuation* of that in the previous interval. This will not be true in the nonlinear case, but nevertheless provides a good starting value for the optimisation. The following lemma provides the appropriate information.

Lemma 1 (Trajectory continuation). If $U^*(\tau)$ is given by Eq. (25) and the control weighting function U(t) at time $t = (k+1)T_{ol}$ is related to that at time $t = kT_{ol}$ by Eq. (32)

$$U((k+1)T_{ol}) = e^{A_u^T T_{ol}} U(kT_{ol})$$
(32)

then the control trajectory within the (k + 1)th open-loop interval is the continuation of the trajectory in the previous interval in the sense that

$$u^{\star}((k+1)T_{ol}, \tau) = u^{\star}(kT_{ol}, \tau + T_{ol}).$$
 (33)

Proof. Using Eqs. (24) and (25), it follows that

$$u^{\star}(kT_{ol}, \tau + T_{ol}) = U_0^{\mathsf{T}} e^{A_u^{\mathsf{T}}(k+1)T_{ol}} U(kT_{ol})$$
(34)

$$= U_0^{\mathsf{T}} e^{A_u^{\mathsf{T}} k T_{ol}} e^{A_u^{\mathsf{T}} T_{ol}} U(k T_{ol}). \tag{35}$$

The result follows using Eq. (32). \Box

To summarise: parts (1) and (2) of the algorithm of Table 1 are executed *in parallel* every T_{ol} seconds. Part (1) of the algorithm is the open-loop control; and part (2) of the algorithm updates the state and parameter estimates together with the control weights for the *next* iteration. The iteration is indexed by k.

5. Example

A commercial laboratory inverted pendulum system described by Apkarian (1995) is pictured in Fig. 3(a). This example was chosen for a number of reasons: the system is nonlinear, the system is nonsquare (two output, one input) and its dynamics, though complex, can be readily captured by the bond graph approach.

As a typical mechatronic system, some parameters are known and some are not. Table 2 shows a list of the relevant physical parameters of this system. Apart from the three friction parameters $(f_a, f_c \text{ and } f_p)$ these parameters are all listed in the system manual and, where appropriate were checked by direct measurements on the component parts of the system.

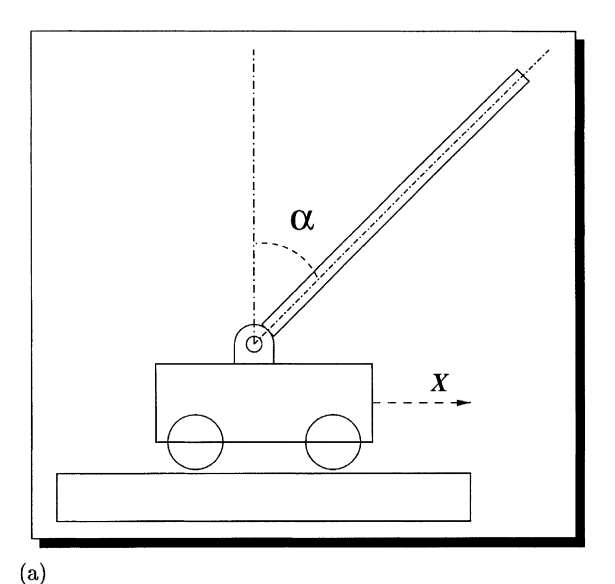
The construction of the system was such that the friction at the joint of the pendulum was negligible. The remaining friction coefficients were estimated from *measured data* using the methods of Section 4.2 as described in Section 5.2.

The system is designed for using simple *linear* control techniques and the pendulum angle is restricted to lie within a small distance from vertical and the system is therefore incapable of large movements. Hence, the properties of the non-linear predictive pole-placement

Table 1
The algorithm

- (1) Compute the open-loop control using the *predefined* $U^*(\tau)$ together with $U(kT_{ol})$ computed at iteration k-1: $u(\tau + kT_{ol}) = U^*(\tau)U(kT_{ol}) \tag{36}$
- (2) Compute $U((k+1)T_{ol})$:

 (a) Using output data from the *previous* interval $((k-1)T_{ol} \le t < kT_{ol})$, and the previously estimated "initial" state use the method of Section 4.2 to estimate the system "initial" state at $t = (k-1)T_{ol}$ and, optionally, system parameters.
 - (b) Use to model to compute the *current* state at $t = kT_{ol}$.
 - (c) Use to model to compute the *predicted* state at $t = (k + 1)T_{ol}$.
 - (d) Use the continuation trajectory condition (Eq. (32)) to compute a starting value for the PPP optimisation.
 - (e) Using the *predicted* state, together with estimated system parameters and the model, use the method of Section 4.1 to compute the control weighing function $U((k+1)T_{ol})$ for the *next* algorithm iteration.



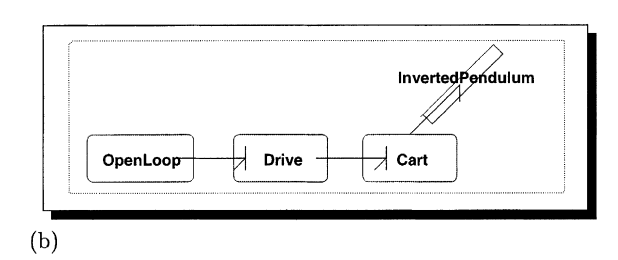


Fig. 3. The inverted pendulum on a cart; (a) schematic, (b) word bond graph.

algorithm are demonstrated using a *simulated* version of the model of the system in Section 5.3.

5.1. Bond graph model

Bond graph modelling is a well-established technique and a number of textbooks exist including those of

Table 2 Physical parameters

Parameter	Units	Value	Description
$\begin{array}{c} l_a \\ j_a \\ r_a \\ f_a \\ k_g \\ r \\ m_c \\ f_c \\ m_p \\ l_p \\ j_p \end{array}$	H kg m² Ω N/m s None m kg N/m s kg m kg m²	0.18e - 3 3.87e - 7 2.6 Unknown 1/3.7 0.635e - 2 0.7429 Unknown 0.210 0.61m $\frac{1}{12}m_pl_p^2$	Motor armature inductance Motor armature inertia Motor armature resistance Motor armature friction Motor gear ratio Cart wheel radius Cart mass Cart friction Pendulum mass Pendulum length Pendulum inertia
f_p	kg m ²	Negligible	Pendulum friction

Karnopp et al. (1990), Thoma (1990), Cellier (1991), and Gawthrop and Smith (1996). To avoid unnecessary details, the *word* bond graph of the higher levels of the system is presented in Fig. 3(b) and the word bond graph of two of the subsystems in Fig. 4. The open-loop control bond graph (see Section 4.1) appears in Fig. 2. The system nonlinearities arise from the angle-modulated transformers of Karnopp (1969) corresponding to the kinematic transformations inherent in the inverted pendulum problem. The details of the pendulum model are the same as presented by Gawthrop and Smith (1996).

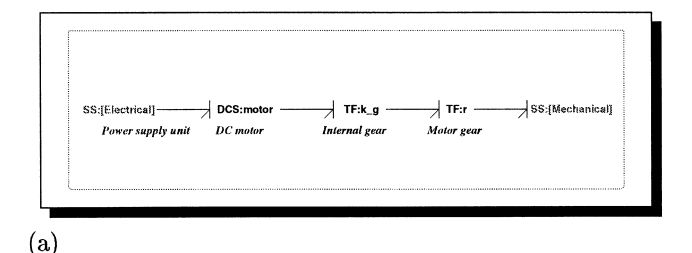
The resulting system has five states (the pendulum angle and angular momentum, the cart position and momentum and the motor armature current). The pendulum model contains a number of *I* components in derivative causality and, as discussed by Gawthrop and Smith (1996), this leads to constrained-state equations in this case corresponding to the system *inertia matrix*.

The corresponding sensitivity system has 10 states as was automatically generated from the system bond graph using the software MTT (MTT, 2000) which also generated code in the C language to be compiled and executed ready for generating the sensitivity functions to be used in the optimisations and simulations.

The algorithm of Table 1 was coded in Octave (Octave, 1999) and used to generate the figures using a Toshiba laptop running GNU/Linux (GNU, 1999).

5.2. Friction estimation

It appears from the experiments reported here that a linear friction model suffices. However, the method can be readily extended to more sophisticated friction models, for example those of Hirshorn and Miller (1999) and Canudas de Wit, Olsson, Astrom and Lischinsky (1995). Within this context, there are two unknown friction



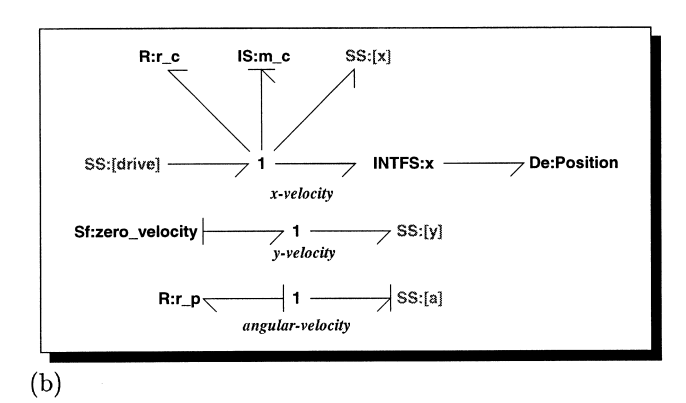


Fig. 4. Subsystems: word bond graph; (a) drive subsystem, (b) cart subsystem.

coefficients f_a and f_c . As far as the system output is concerned, these two friction coefficient may be replaced by 0 and $r_c = f_c + (1/(rk_g)^2)f_a$. Thus, for the purposes of control, only the single coefficient r_c needs to be measured.

Input output data was gathered for the cart with the pendulum removed. Fig. 5(a) shows the system input (V) and the system output (m) plotted against time (s). These data were used in the algorithm of Section 4.2 and both r_c and the three initial system states were estimated. Fig. 5(b) shows the estimated value of r_c plotted against the iteration number. Convergence takes about three iterations. Note that, in this context, the value of the initial system states are not of any interest. However, it is necessary to estimate them to fit the data correctly. The estimated value of r_c is

$$\hat{r}_c = 7.198 \,\text{N/m s.}$$
 (37)

Two advantages of the physically based estimation approach are illustrated by this experiment. Estimation can take place on *part* of the overall system, and the known physical data is fully used.

5.3. Predictive control

A number of simulations of the model of Section 5.1, using the parameters of Table 2 together with Eq. (37), were made to verify the properties of the algorithm. The basic controller parameters are (unless otherwise stated) given in Table 3. The corresponding basis functions $U^*(\tau)$

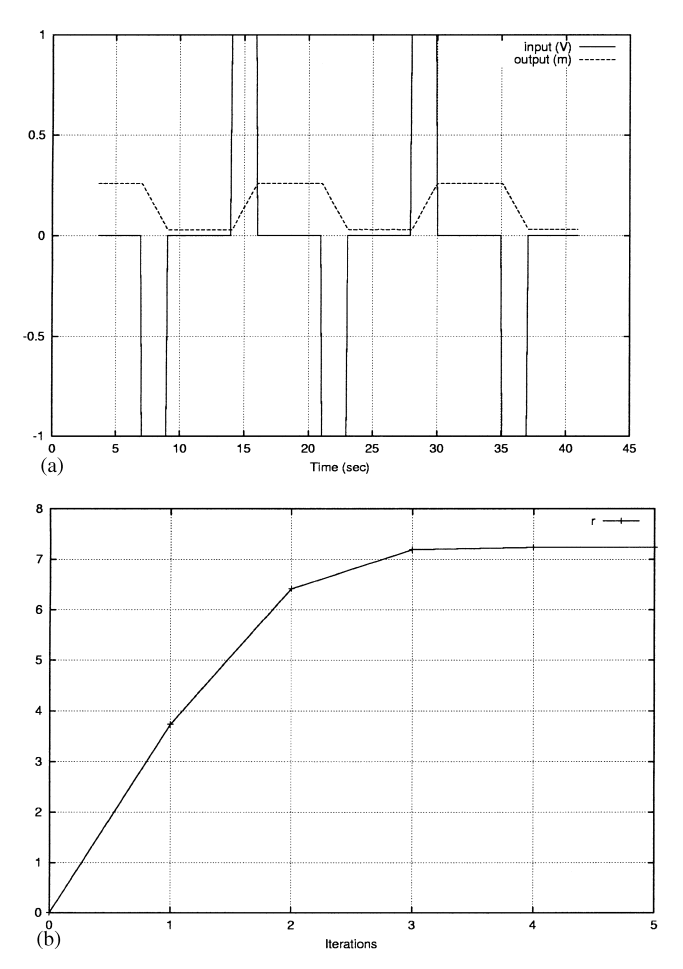


Fig. 5. Estimating the cart friction; (a) data, (b) estimated r_c .

Table 3 Controller parameters

Name	Symbol	Value
Input time constant	T_U	0.02 s
Number of basis functions	n_U	4
Open-loop interval	T_{ol}	0.1 s
Sample interval	T_s	0.005 s
Lower optimisation horizon	$ au_1$	0.8 s
Upper optimisation horizon	$ au_2$	1.0 s
Angle setpoint	w_{α}	0.0
Position setpoint	w_X	0.0

were the first four (unormalised) Laguerre functions of Fig. 6 corresponding to

$$A_{u} = -\frac{1}{T_{U}} \begin{pmatrix} 1 & 0 & 0 & 0 \\ 2 & 1 & 0 & 0 \\ 2 & 2 & 1 & 0 \\ 2 & 2 & 2 & 1 \end{pmatrix}, \tag{38}$$

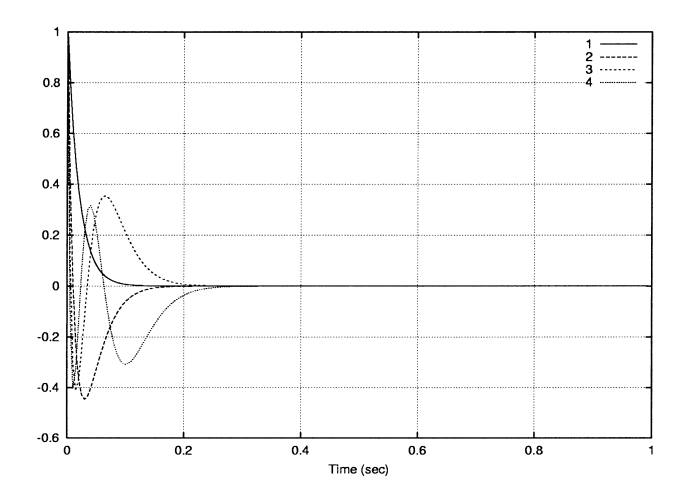
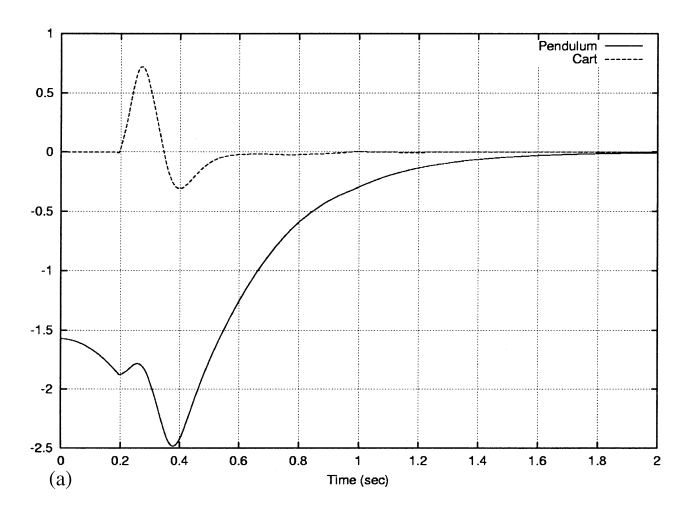


Fig. 6. The basis functions U^* .



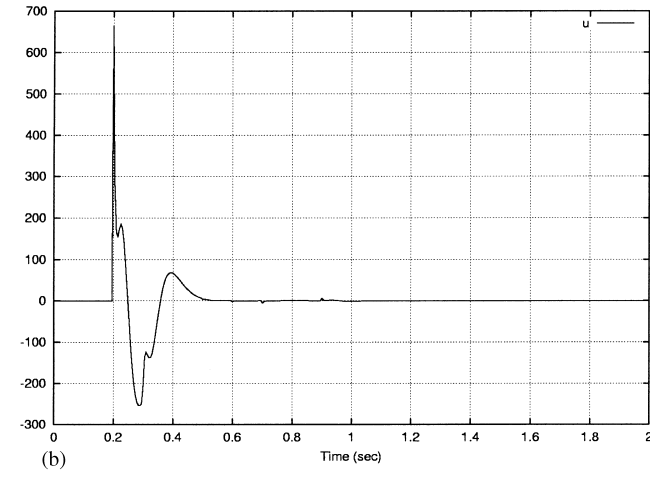


Fig. 7. Regulation from $\theta = \pi/2$; (a) pendulum and cart positions, (b) control.

where T_U is given in Table 3. In all cases, regulation from an initial horizontal pendulum position to a vertical pendulum position with an incorrect initial state estimate is used; this is a demanding control problem.

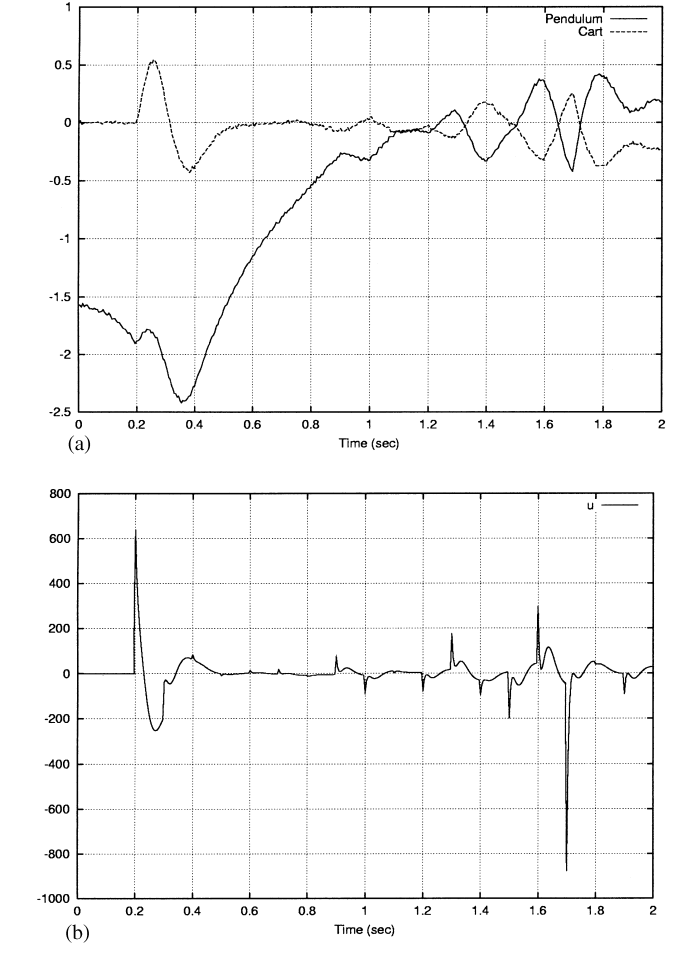


Fig. 8. Regulation from $\theta=\pi/2$ with noise; (a) pendulum and cart positions, (b) control.



Fig. 7(a) shows the two system outputs (X and α), and Fig. 7(b) the corresponding control signal (motor voltage). The initial angle of the inverted pendulum is $\alpha = -\pi/2$ (pendulum horizontal), but the model initially assumes $\alpha = 0$. For the latter reason, no control action is taken during the initial control interval $t < T_{ol} = 0.2$ and the pendulum drops further. Based on these data, and in the absence of measurement noise, the state estimator obtains an accurate estimate of the state which is used as the basis for the subsequent control actions. At the end of the simulation, both outputs are close to the setpoints of zero (pendulum vertical, centre track). The control signal is considerably outside the specified maximum of \pm 10 V; this is indicative of the fact noted above that the system design is unsuitable for this large motion.

Fig. 8 is same as Fig. 7 except that Gaussian white measurement noise of standard deviation 0.01 is added to each output. This causes some deviation from the ideal situation, but a stable result is still achieved.

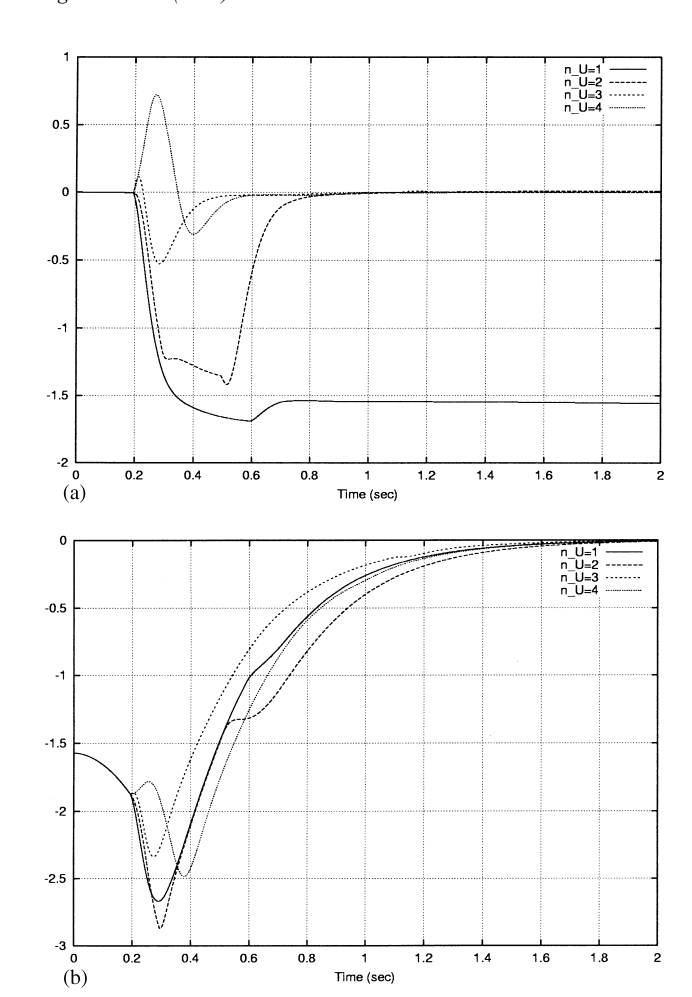


Fig. 9. Effect of number of basis functions n_U ; (a) cart position, (b) pendulum position.

Fig. 9 illustrates the same simulation as Fig. 7 but with four different values of $n_U = 1 - 4$. For clarity, the Cart position is displayed separately (part (a)) from the Pendulum position (part (b)). $n_U = 4$ corresponds exactly to the situation of Fig. 7, the other three plots display the effect of reducing the number of basis functions. Roughly speaking, $n_U = 3$ gives little loss in performance, whilst smaller values of n_U are unsatisfactory.

Fig. 10 shows the number of optimisation iterations required to evaluate the control weights U(t) at each step. Three graphs are shown. Those marked "Nonlinear" and "Nonlinear with noise" correspond to Figs. 7 and 8 respectively, that marked "Linear" corresponds to a simulation identical to that of Fig. 7 except that the initial angle is $\alpha = -\pi/100$ and thus the system is essentially linear. Except for the first iteration, the linear case requires the minimum of 2 iterations indicating a linear/quadratic optimisation. The nonlinear case requires over 40 iterations for the first nontrivial optimisation (t=0.2) but thereafter requires less than 10 indicating that the trajectory continuation method of Lemma 1 is

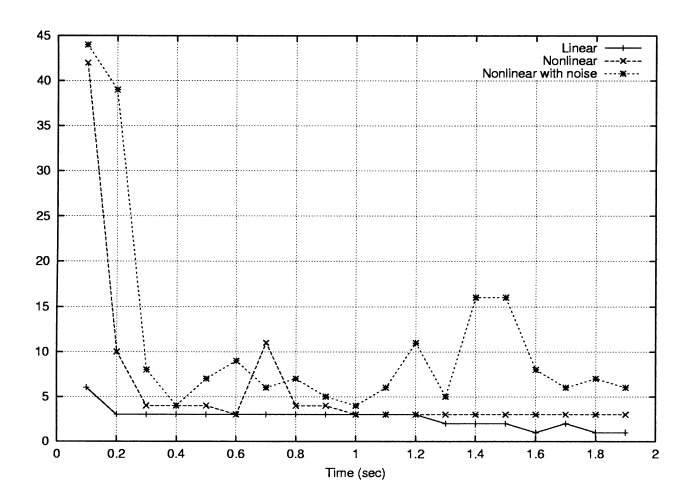


Fig. 10. Optimisation iterations.

effective. The noisy case requires more iterations as the estimated state and predicted states are different.

6. Conclusion

It has been shown that bond graph models of dynamic systems in general, and mechatronic systems in particular, can be used to generate sensitivity information in a form appropriate for optimisation, and that this optimisation can be used for real-time identification, state estimation and control of nonlinear systems which have a bond graph representation.

Although the results of Section 5.2 are based on real data, because of the limitations of the equipment it was not possible to perform the swing-up experiment. However, the simulations of Section 5.3 were based on the verified model and are therefore believed to provide evidence of the applicability of this approach.

Making use of appropriate software tools, this approach provides a powerful way of facilitating the design of mechatronic and other control systems. It is planned to extend the software using the real-time Linux kernel to provide the seemless environment mentioned in the Introduction.

Future work will include extension of the analysis of the linear PPP algorithm to the nonlinear case; performing experiments on real mechatronic systems and experimental comparison with other approaches.

Acknowledgements

This work was accomplished whilst the first author was a visitor at the Centre for Integrated Dynamics and Control, University of Newcastle, New South Wales; he would like to thank Prof. Graham Goodwin for providing an excellent work environment. Dr Will Heath of the

University of Newcastle and Dr Tomas McKelvey of the University of Linköping provided insights into optimisation methods. He would also like to thank Prof. David Murray-Smith of Glasgow University for introducing me to sensitivity methods and Prof. Job Van Amerongen of the University of Twente, for helpful discussions.

Both authors would like to thank Prof. David Hill of the University of Sydney for providing the experimental facilities.

EPSRC support this work through the grant Physically orientated nonlinear control.

References

An, C. H., Atkeson, C. G., & Hollerbach, J. M. (1988). *Model-based control of robot manipulators*. Cambridge, MA: The MIT Press.

Apkarian, J. (1995). A comprehensive and modular laboratory for control systems design and implementation. Markham, Ont.: Quanser Consulting.

Ascend, (1999). Ascend: A flexible modelling environment for hard engineering and science problems. Online WWW Home Page. URL: http://www.cs.cmu.edu/ascend/.

Cabanellas, J. M., Felez, J., & Vera, C. (1995). A formulation of the sensitivity analysis for dynamic systems optimisation based on pseudo bond graphs. In F.E. Cellier, & J.J. Granda, Proceedings of the 1995 international conference on bond graph modeling and simulation (ICBGM'95), Simulation series, vol. 27 (pp. 135–144). Las Vegas, USA: Society for Computer Simulation.

Calahan, D. A. (1972). Computer-aided network design. New York: McGraw-Hill.

Canudas de Wit, C. (1988). Adaptive control for partially known systems. Amsterdam: Elsevier.

Canudas de Wit, C., Olsson, H., Astrom, K. J., & Lischinsky, P. (1995).
A new model for control of systems with friction. *IEEE Transactions on Automatic Control*, 40(3), 419–425.

Cellier, F. E. (1991). Continuous system modelling. Berlin: Springer.

Chen, H., & Allgöwer, F. (1998). A quasi-infinite horizon nonlinear model predictive control scheme with guaranteed stability. *Automatica*, 34(10), 1205–1217.

Clarke, D. W. (1994). Advances in model-based predictive control. Oxford: Oxford University Press.

Dasgupta, S., Anderson, B. D. O., & Kaye, R. J. (1986). Output error identification methods for partially known systems. *International Journal of Control*, 43(1), 177–191.

Demircioglu, H., & Gawthrop, P. J. (1991). Continuous-time generalised predictive control. Automatica, 27(1), 55-74.

Eykhoff, P. (1974). System identification. New York: Wiley.

Fletcher, R. (1987). Practical methods of optimization (2nd ed.). Chichester: Wilev.

Frank, P. M. (1978). *Introduction to system sensitivity theory*. New York: Academic Press.

Gawthrop, P. J. (1995a). Bicausal bond graphs. In F.E. Cellier, & J.J. Granda, Proceedings of the 1995 international conference on bond graph modeling and simulation (ICBGM'95), Simulation series, vol. 27 (pp. 83–88). Las Vegas, USA: Society for Computer Simulation.

Gawthrop, P. J. (1995b). Physical model-based control: A bond graph approach. *Journal of the Franklin Institute*, 332B (3), 285–305.

Gawthrop, P. J., & Smith, L. P. S. (1996). Metamodelling: Bond graphs and dynamic systems. Hemel Hempstead, Herts, England: Prentice-Hall.

Gawthrop, P. J., Demircioglu, H., & Siller-Alcala, I. (1998). Multivariable continuous-time generalised predictive control: A state-space approach to linear and nonlinear systems. *Proceedings of the IEE Part D*, 145(3), 241–250.

- Gawthrop, P. J., Ježek, J., Jones, R. W., & Sroka, I. (1993). Grey-box model identification. Control-Theory and Advanced Technology.
- Gawthrop, P. J., Jones, R. W., & MacKenzie, S. A. (1992). Identification of partially-known systems. *Automatica*, 28(4), 831–836.
- Gawthrop, P. J. (2000). Sensitivity bond graphs. *Journal of the Franklin Institute*, submitted for publication.
- Gawthrop, P. J., & Ronco, E. (1999). Predictive pole-placement control with linear models. *Automatica*, submitted for publication.
- GNU, (1999). Gnu home page. Online WWW. URL: http://www.gnu.org.
- Hirshorn, R. M., & Miller, G. (1999). Control of nonlinear systems with friction. *CST*, 7(5), 588–595.
- Karnopp, D. C. (1969). Power-conserving transformations: Physical interpretations and applications using bond graphs. *Journal of the Franklin Institute*, 288(3), 175–201.
- Karnopp, D. C. (1979). Bond graphs in control: Physical state variables and observers. *Journal of the Franklin Institute*, 308(3), 221–234.
- Karnopp, D. C. (1995). Actively controlled systems: An ideal application area for bond graph modelling (plenary address). In F. E. Cellier, & & J.J. Granda, *Proceedings of the 1995 international conference on bond graph modeling and simulation (ICBGM'95)* (p. 3). Las Vegas, USA: Society for Computer Simulation.
- Karnopp, D. C., Margolis, D. L., & Rosenberg, R. C. (1990). System dynamics: A unified approach. New York: Wiley.
- Karnopp, D. (1977). Power and energy in linearised systems. *Journal of the Franklin Institute*, 303(1), 85–98.
- Kouvaritakis, B., Cannon, M., & Rossiter, J. A. (1999). Non-linear model-based predictive control. *International Journal of Control*, 72(10), 919–928.
- Modelica, (2000). Modelica: Language design for multi-domain modeling. Online WWW Home Page. URL: http://www.modelica.org/.

- MTT, (2000). MTT: Model transformation tools. Online WWW Home Page. URL: http://www.eng.gla.ac.uk/peterg/ software/MTT/.
- Muske, K. R., & Rawlings, J. B. (1993). Model predictive control with linear models. *Process Systems Engineering*, 39(2), 262–287.
- Octave, (1999). Octave home page. Online WWW. URL: http://www.che.wisc.edu/octave/.
- Oppen, I., Gong, M., & Murray-Smith, D. J. (1995). The development of tuning techniques for single-input single-output and multivariable control systems using controller sensitivity measures In: R.C.H. Cheng, & R.J. Pooley, UKSS'95 Second Conference of the UK Simulation Society (pp. 73–79). Edinburgh, UK: UKSS.
- Press, W. H., Teukolsky, S. A., Vetterling, W. T., & Flannery, B. P. (1992). Numerical recipes in C. (2nd ed.). Cambridge: Cambridge University Press.
- Ronco, E., Arsan, T., & Gawthrop, P. J. (1999). Open-loop intermittent feedback control: Practical continuous-time GPC. *IEE Proceedings* Part D, 146(5), 426–434.
- Ronco, E., & Gawthrop, P. J. (1999). Symbolic quasi-Newton optimisation for system identification. Proceedings of the UKACC conference on "Control 2000". Cambridge, UK.
- Thoma, J. U. (1990). Simulation by bond graphs. Berlin: Springer.
- Tomović, R., & Vukobratović, M. (1972). Modern analytic and computational methods in science and mathematics, General sensitivity theory, vol. 35. New York: Elsevier.
- Van Amerongen, J., & Udink ten Cate, A. J. (1975). Model reference autopilots for ships. *Automatica*, 11, 441-449.
- Winning, D. J., El-Shirbeeny, E. H. T., Thompson, E. C., & Murray-Smith, D. J. (1977). Sensitivity method for online optimisation of a synchronous generator excitation controller. *Proceedings IEE Part* D, 124(7), 631–638.